

Purdue University Purdue e-Pubs

School of Mechanical Engineering Faculty
Publications

School of Mechanical Engineering

2006

A constitutive model of the human vocal fold cover for fundamental frequency regulation

Kai Zhang
Purdue University

Thomas Siegmund
Purdue University, siegmund@purdue.edu

Roger W. Chan
University of Texas Southwestern Medical Center

Follow this and additional works at: <http://docs.lib.purdue.edu/mepubs>

 Part of the [Mechanical Engineering Commons](#)

Recommended Citation

Zhang, Kai; Siegmund, Thomas; and Chan, Roger W., "A constitutive model of the human vocal fold cover for fundamental frequency regulation" (2006). *School of Mechanical Engineering Faculty Publications*. Paper 8.
<http://docs.lib.purdue.edu/mepubs/8>

This document has been made available through Purdue e-Pubs, a service of the Purdue University Libraries. Please contact epubs@purdue.edu for additional information.

A constitutive model of the human vocal fold cover for fundamental frequency regulation

Kai Zhang and Thomas Siegmund^{a)}

School of Mechanical Engineering, Purdue University, 585 Purdue Mall, West Lafayette, Indiana 47907

Roger W. Chan

Otolaryngology – Head and Neck Surgery, and Biomedical Engineering, University of Texas Southwestern Medical Center, Dallas, Texas 75390-9035

(Received 4 April 2005; revised 10 October 2005; accepted 29 November 2005)

The elastic as well as time-dependent mechanical response of the vocal fold cover (epithelium and superficial layer of the lamina propria) under tension is one key variable in regulating the fundamental frequency. This study examines the hyperelastic and time-dependent tensile deformation behavior of a group of human vocal fold cover specimens (six male and five female). The primary goal is to formulate a constitutive model that could describe empirical trends in speaking fundamental frequency with reasonable confidence. The constitutive model for the tissue mechanical behavior consists of a hyperelastic equilibrium network in parallel with an inelastic, time-dependent network and is combined with the ideal string model for phonation. Results showed that hyperelastic and time-dependent parameters of the constitutive model can be related to observed age-related and gender-related differences in speaking fundamental frequency. The implications of these findings on fundamental frequency regulation are described. Limitations of the current constitutive model are discussed. © 2006 Acoustical Society of America.
[DOI: 10.1121/1.2159433]

PACS number(s): 43.70.Aj, 43.70.Bk [AL]

Pages: 1050–1062

I. INTRODUCTION

In an understanding of voice production processes it is of great interest to obtain predictions of the fundamental frequency of phonation F_0 and to compare such model predictions to experimentally determined trends. Intrinsically, the fundamental frequency of phonation is dependent on the mechanical properties of the tissue in the vocal fold. Specifically, the human vocal fold cover, or superficial layer of the lamina propria, is predominantly an extracellular matrix (ECM) that is optimally designed for tissue vibration and sound production in response to a unique set of biomechanical stimuli in the human larynx. These stimuli include small-strain deformation due to small-amplitude vibration of the vocal fold as well as large-strain deformation due to vocal fold posturing.¹ Small strain deformation occurs at high magnitudes of acceleration (up to 200–300 g) and at high frequencies (around 100–150 Hz for male voice, 200–300 Hz for female voice).² Large strain deformation occurs at low frequencies (around 1–10 Hz) and is relevant to vocal fold posturing, i.e., the processes of vocal fold length changes and abduction/adduction creating an optimal set of vocal fold shape and glottal geometry, in order to achieve a desired mode of vibration and vocal fundamental frequency.¹ Vocal fold length adjustments during posturing are primarily driven by the antagonistic actions between cricothyroid and thyroarytenoid muscle activities, resulting in a large strain deformation at tensile strains ranging from 0 to over 40%, or

perhaps over 50%. Such high magnitudes of strain are found in situations where singers need to go up the musical scale by more than two octaves. Specific levels of deformation depend on the actual desired fundamental frequency, the relationship between the amplitude of vocal fold vibration and the vocal fold length, and the subglottal pressure.³ These length changes in the vocal fold are related to the stress level in the vocal fold through the mechanical response of the vocal fold tissue. Furthermore, it is of interest to obtain an understanding of the time course of fundamental frequency changes during speech $F_0(t)$ where t is time. Experimental data on the large-strain mechanical response of vocal fold tissue clearly demonstrate a nonlinear time-dependent behavior.⁴ Due to this inherent viscous nature of the vocal fold tissue, the time-dependent changes in vocal fold length are directly linked to changes in fundamental frequency. For an understanding of these phenomena from a continuum mechanics perspective, a constitutive model that reliably describes the stress-strain response of tissues in the vocal fold is of importance. Specifically, the focus of the present study is to investigate fundamental frequency predictions under consideration of a large-strain time-dependent tensile stress-strain response of the vocal fold cover. In the past vocal fold tissue has commonly been described by either linear elastic models,^{5,6} nonlinear elastic models,^{7–10} or viscoelastic models through the introduction of multiple relaxation times or a time dependence of the elastic constants.^{1,11,12} These models possess limitations in dealing with the highly nonlinear tissue response, especially in the large-strain time-dependent response. In the present paper the constitutive description is based on the idea of network models¹³ formulated within an

^{a)} Author to whom correspondence should be addressed. Electronic mail: siegmund@ecn.purdue.edu

inelastic and time-dependent continuum constitutive relation such that the tissue response to any load is the outcome of an increment solution. For the description of the hyperelastic response of the tissue the Ogden model¹⁴ is used, which has been shown to be promising in the characterization of the tensile behavior of other soft tissues, e.g., brain tissue.^{15,16} In addition, a flow rule^{17,18} is defined which correlates stress and strain to the magnitude of the time-dependent inelastic deformation. Models of this type have been shown to be capable of describing a wide range of experimentally observed effects in the mechanical behavior of polymers^{17–20} and soft tissues.^{18,21,22}

The model is applied to results of measurements of the tensile mechanical properties of vocal fold cover specimens obtained from human subjects. Through the constitutive model one can then establish a link between the tissue constitutive properties and histological structure of the vocal fold lamina propria. This provides insights into the relationship between tissue structure and tissue function. Specifically, the present study attempts to correlate the relative densities of collagen and elastin fibers in the vocal fold reported in the literature, including their age-related and gender-related differences,^{23,24} with age- and gender-related changes in the parameters of the constitutive model, and finally empirical age- and gender-related dependencies of the fundamental frequency. Even with the number of available human subjects being limited, preliminary conclusions are drawn which correlated well with empirical data on speaking fundamental frequency changes.

II. MECHANICS OF F_0 REGULATION

A. The string model

The ideal string model of phonation³ provides the starting point for the investigation of the fundamental frequency of phonation. In this model an ideal undamped situation is assumed, and F_0 can be expressed as a function of the current vocal fold length l , the tissue density ρ , and the tissue longitudinal stress σ :

$$F_0 = \frac{1}{2l} \sqrt{\frac{\sigma}{\rho}}. \quad (1)$$

Recently, Titze and Hunter²⁵ showed that the string model described by Eq. (1) may underestimate the fundamental frequencies of the vocal fold, specifically the vocal ligament, especially at low ranges of strain. By taking into account the effects of variable cross-sectional area and bending stiffness of the vocal fold macula flavae they derived an empirical correction rule to correct the ideal string model as

$$F_0 = \frac{1}{2l} \sqrt{\frac{\sigma}{\rho}} [1 - 0.45 \ln(\lambda_u - 1)]. \quad (2)$$

With this correction, the fundamental frequency is dependent on the magnitude of deformation applied due to posturing. Throughout the present study, deformation is measured as stretch λ . In a uniaxial loading condition, stretch is defined as $\lambda_u = 1 + \epsilon = l/L$, with $\epsilon = (l/L) - 1$ being strain and L being

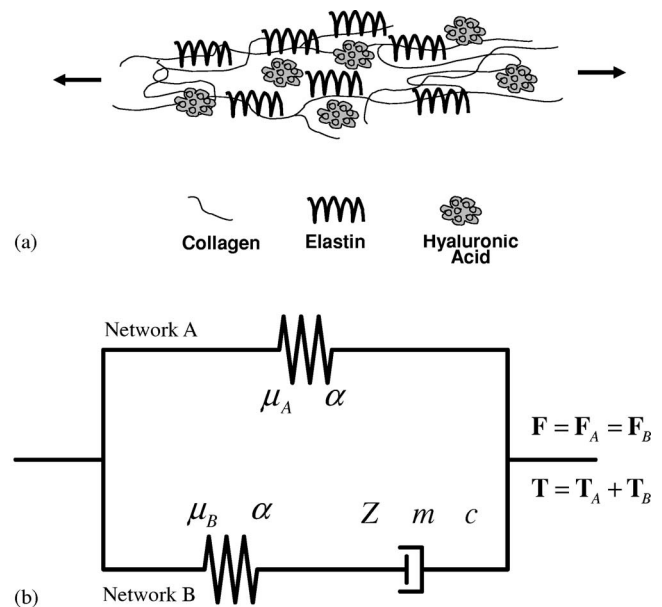


FIG. 1. (a) A schematic representation of molecular networks in the vocal fold extracellular matrix (ECM) following Ref. 26. (b) A one-dimensional rheological representation of the constitutive model, with a hyperelastic equilibrium network (A) in parallel with an inelastic network (B).

the resting length of the vocal fold. Equation (2) was defined to be valid in the range of $\lambda_u = 1.1$ to 1.5 .²⁵

In the following, we focus on implications of the constitutive model describing tissue deformation on fundamental frequency regulation. Such effects can be revealed by combining the string models of Eqs. (1) and (2) with an appropriate constitutive model of the vocal fold tissue.

B. A constitutive model for the vocal fold cover

The use of a network-type constitutive model is motivated by the underlying tissue structure. Following Gray *et al.*,^{26,27} Fig. 1(a) depicts a schematic representation of the molecular networks present in the ECM of the vocal fold lamina propria. The main constituents include networks of fibrous proteins (collagen and elastin) and water-absorbing, space-occupying hyaluronic acid molecules. Mechanically, the fibrous proteins collagen and elastin provide a structural framework, whereas hyaluronic acid and other interstitial protein molecules contribute to regulate the viscosity and elasticity of the ECM.^{26,27} Reflecting this molecular structure, the constitutive model consists of a time-independent equilibrium network (A) in parallel with a time-dependent network (B) [Fig. 1(b)]. No specific assumption is made with regard to collagen, elastin, or interstitial protein molecules exclusively contributing to either network considered in the model. Instead, both the equilibrium response and the inelastic response are assumed to arise from molecular interactions between connected network components, among collagen, elastin, or other protein molecules. In the following, the constitutive model is described in a complete three-dimensional formulation. However, in view of the string model [Eq. (1)], appropriate one-dimensional relationships are given.

The deformation gradient \mathbf{F} relates the length and orientation of a material element $d\mathbf{X}$ in the reference configuration

to its length and orientation in the deformed configuration $d\mathbf{x}$ through $d\mathbf{x} = \mathbf{F} \cdot d\mathbf{X}$. Initial length and current length are defined as $(dL)^2 = d\mathbf{X}^T \cdot d\mathbf{X}$ and $(dl)^2 = d\mathbf{x}^T \cdot d\mathbf{x}$, respectively, so that stretch λ is

$$\lambda^2 = \frac{d\mathbf{x}^T \cdot d\mathbf{x}}{d\mathbf{X}^T \cdot d\mathbf{X}} = \mathbf{N}^T \cdot \mathbf{F}^T \cdot \mathbf{F} \cdot \mathbf{N} \quad (3)$$

in which \mathbf{N} is the unit vector along the orientation of $d\mathbf{X}$.

The two networks (A) and (B) are in parallel with each other such that the applied deformation gradient \mathbf{F} is identical to the deformation gradients in the networks, $\mathbf{F}_A, \mathbf{F}_B$:

$$\mathbf{F} = \mathbf{F}_A = \mathbf{F}_B. \quad (4)$$

A one-dimensional rheological model representation of the model is given in Fig. 1(b). Following this parallel arrangement of networks, the total Cauchy stress \mathbf{T} is the sum of the Cauchy stresses in networks (A) and (B), $\mathbf{T}_A, \mathbf{T}_B$:

$$\mathbf{T} = \mathbf{T}_A + \mathbf{T}_B. \quad (5)$$

The equilibrium network (A) is characterized by a hyperelastic (large-strain) constitutive behavior. In the analysis of the experimental data it was found that a first-order Ogden model¹⁴ together with the assumption of incompressible material response (with the Poisson's ratio $\nu=0.5$) allows for an appropriate description of the tissue behavior. This model is described by a strain energy density function w of the form¹⁴

$$w = \frac{2\mu_A}{\alpha^2} (\lambda_1^\alpha + \lambda_2^\alpha + \lambda_3^\alpha - 3), \quad (6)$$

where μ_A is the initial shear modulus of the equilibrium network and α is the corresponding dimensionless constant describing the nonlinearity of the elastic response. For incompressible behavior the shear modulus is related to the elastic modulus (Young's modulus, E) with $E=3\mu$. The deformation is characterized through the principal stretches $\lambda_1, \lambda_2, \lambda_3$ which satisfy $\lambda_1\lambda_2\lambda_3=1$. It is recognized that the vocal fold cover may not be completely isotropic in microstructure and thus in its mechanical properties.^{5,11} In the present study, however, effects of anisotropy are not considered.

In the time-dependent network (B), the deformation gradient is decomposed multiplicatively into an elastic component \mathbf{F}^e and a viscoplastic component \mathbf{F}^p :

$$\mathbf{F} = \mathbf{F}_B = \mathbf{F}_B^e \cdot \mathbf{F}_B^p. \quad (7)$$

The elastic response of network (B) is again described by an Ogden model, with initial shear modulus μ_B and the power α . Thus, a formulation identical to that of Eq. (6) introduced for the description of network (A) applies for the elastic part of network (B). In the present model it is assumed that the two networks (A) and (B) possess the same power α in the hyperelastic response but different values of the initial network shear moduli, $\mu_A \neq \mu_B$. Following the formulation in Ref. 17 the inelastic rate of the shape change of network (B) is

$$\tilde{\mathbf{D}}_B^p = \dot{\lambda}_B^p \frac{\mathbf{S}_B}{\bar{\sigma}_B} = \mathbf{F}_B^e \dot{\mathbf{F}}_B^p (\mathbf{F}_B^p)^{-1} (\mathbf{F}_B^e)^{-1}, \quad (8)$$

where \mathbf{S}_B is the deviator of the Cauchy stress tensor in network (B), and $\bar{\sigma}_B = \sqrt{(3/2)\mathbf{S}_B : \mathbf{S}_B}$ is the corresponding effective stress. The inelastic component of the deformation gradient in network (B) is obtained by inverting the relationship $\tilde{\mathbf{D}}_B^p = \mathbf{F}_B^e \dot{\mathbf{F}}_B^p (\mathbf{F}_B^p)^{-1} (\mathbf{F}_B^e)^{-1}$. The effective inelastic stretch rate $\dot{\lambda}_B^p$ depends on the effective inelastic stretch $\bar{\lambda}_B^p$ and the effective stress $\bar{\sigma}_B$:

$$\dot{\lambda}_B^p = Z(\bar{\lambda}_B^p - 1 + \delta)^c (\bar{\sigma}_B)^m. \quad (9)$$

The model introduces three parameters for the description of the inelastic response. The stress exponent m characterizes the dependence of the inelastic deformation on the stress level in network (B). The stretch exponent c ($-1 < c < 0$) characterizes the dependence of the rate of inelastic deformation on the current magnitude of inelastic deformation. The viscosity scaling constant Z defines the absolute magnitude of the inelastic deformation. Furthermore, δ is a small positive number ($\delta < 0.001$) introduced to avoid singularities in the inelastic stretch rate when the inelastic stretch is close to one.¹⁸

For uniaxial loading of a specimen of initial length L to a current length l the principal stretches are $\lambda_1 = \lambda_u, \lambda_2 = \lambda_3 = 1/\sqrt{\lambda_u}$ where $\lambda_u = 1 + \epsilon_u = l/L$. For the equilibrium response as given by the nominal stress in network (A), the total nominal stress $\sigma = \sigma_A$. This stress is obtained as the derivative of the strain energy density w with respect to the applied stretch λ_u :

$$\sigma = \sigma_A = \frac{\partial w}{\partial \lambda_u} = \frac{2\mu_A}{\alpha} (\lambda_u^{\alpha-1} - \lambda_u^{-(1/2)\alpha-1}). \quad (10)$$

Under consideration of the time-dependent response, stress is calculated from the elastic components of stretch λ_A^e, λ_B^e and both depend on the applied stretch λ_u and the applied stretch rate $\dot{\lambda}_u$. For network (A) the elastic stretch rate is $\dot{\lambda}_A^e = \dot{\lambda}_A = \dot{\lambda}_u$ and the elastic stretch is $\lambda_u = \lambda_A = \lambda_A^e$. In network (B) the elastic stretch rate $\dot{\lambda}_B^e$ can be expressed as

$$\dot{\lambda}_B^e = \dot{\lambda}_u \frac{\lambda_B^e}{\lambda_u} - \frac{2}{3} \lambda_B^e \cdot Z \cdot \text{sgn}(\lambda_B^e - 1) \cdot \left\{ \sqrt{\frac{1}{3} \left[\left(\frac{\lambda_u}{\lambda_B^e} \right)^2 + \frac{2\lambda_B^e}{\lambda_u} \right]} - 1 + \delta \right\}^c \cdot \left| \frac{2\mu_B}{\alpha} [(\lambda_B^e)^\alpha - (\lambda_B^e)^{-\alpha/2}] \right|^m \quad (11)$$

with the elastic stretch component λ_B^e found through numerical integration²⁸ of Eq. (11). With these formulations, the total nominal stress σ can be obtained:

$$\sigma = \frac{2\mu_A}{\alpha} [\lambda_u^{\alpha-1} - \lambda_u^{-\alpha/2-1}] + \frac{2\mu_B}{\alpha} [(\lambda_B^e)^{\alpha-1} - (\lambda_B^e)^{-\alpha/2-1}]. \quad (12)$$

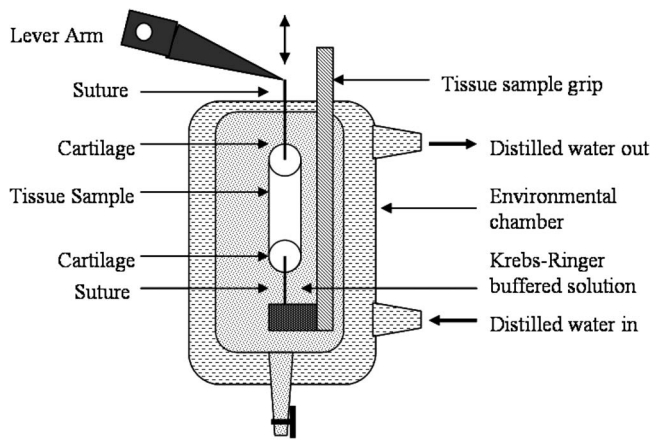


FIG. 2. Schematic of the experimental setup for uniaxial tensile stretch-release test of vocal fold tissues using a dual-mode servo-control lever system.

III. TISSUE DATA

A. Experimental method

The passive uniaxial tensile stress-strain response of the human vocal fold cover was measured by sinusoidal stretch-release (loading-unloading), with the use of a dual-mode servo control lever system (Aurora Scientific Model 300B-LR, Aurora, ON) (Fig. 2). The servo control lever system allowed for precise real-time measurements of the displacement and force of the lever arm, with a displacement accuracy of $1.0 \mu\text{m}$ and a force resolution of 0.3 mN . The servo-control lever system possessed a displacement range of up to $8\text{--}9 \text{ mm}$ in the frequency range of $1\text{--}10 \text{ Hz}$. The experimental protocol was approved by the Institutional Review Board of UT Southwestern Medical Center.

The sinusoidal tensile stretch-release protocol for obtaining stress-strain data was similar to those of Alipour and Titze⁷ and Perlman,²⁹ but the dissection was different because only canine vocal fold tissues were tested in those previous studies, instead of human. In the present study, the vocal fold cover, i.e., the epithelium and the superficial layer of the lamina propria, was dissected with instruments for phonomicrosurgery, as summarized in Chan and Titze¹¹ (please note that in Chan and Titze¹¹ the vocal fold cover was referred to as the “mucosa”). In particular, the superficial layer of the lamina propria was separated from the intermediate layer (the vocal ligament) and the thyroarytenoid muscle (the vocal fold body) by a Bouchayer spatula for blunt dissection. This lateral boundary of excision was facilitated by the natural plane of dissection between the superficial layer and the middle layer of the lamina propria, which was correlated to elastin fiber density.³⁰ No muscle tissue was observed in all of the vocal fold cover specimens isolated. Each cover specimen remained naturally attached to a small portion of thyroid cartilage at the anterior end and a small portion of arytenoid cartilage at the posterior end, to which sutures were attached for mounting and for elongation. It is believed that the tissue primarily responsible for bearing stress and undergoing deformation was the cover itself (epithelium and/or superficial layer of the lamina pro-

pria), since the vocal ligament and the vocal fold body (muscle) were excluded from the specimen after dissection.

Each vocal fold cover specimen to be tested was mounted vertically to the lever arm through sutures in Krebs-Ringer solution at a pH of 7.4 and at 37°C in a glass environmental chamber. In all experiments the loading rate was 1 Hz . This frequency for vocal fold length changes was selected based on the following considerations. A broad range of speeds of vocal pitch changes was observed in human subjects^{31,32} and in canines *in vivo*.³³ A response time of around $50\text{--}100 \text{ ms}$ was found for human singers and untrained subjects as they attempted ascending and descending pitch jumps at maximum speeds.^{31,32} A time constant of about 30 ms was found for exponential increase or decrease in vocal fold strain in dogs under supramaximal electrical stimulation of the superior laryngeal nerve or the recurrent laryngeal nerve, up to a maximum positive strain (elongation) of about 45% .³³ The exponential time constant observed in the canine study was consistent with the human response time, as it was defined as reaching 66.7% of the target pitch, while it would take about three time constants (90 ms) to approach steady state.³³ A time constant of 50 ms would correspond to a loading rate of 10 Hz for 50% vocal fold elongation under sinusoidal deformation, whereas 500 ms would correspond to a loading rate of 1 Hz . Since the vocal fold length changes in these experiments were executed at maximum speeds or supramaximally, for lower speeds of pitch changes such as those during speech, particularly for males, the time constant could approach 500 ms , i.e., a loading rate of 1 Hz as chosen in the present experiments.

Displacement and tensile force of the specimen under cyclic stretch-release were measured, and data were acquired at a sampling rate of 1000 samples per second per channel with a 14-bit signal amplitude resolution. From the vocal fold *in situ* length (resting cadaveric length) L and the current length l the uniaxial stretch of a specimen was obtained as $\lambda_u = l/L$. The nominal tensile stress σ was determined from the measured force divided by the specimen cross-sectional area A , estimated by $A = M/(\rho L)$ where M is the mass of the specimen.⁷ The mass of each cover specimen was measured after the completion of the tensile stretch-release experiment. A possible hydration-induced change in mass of the specimens in the present study was not examined, but results of an animal model showed that the mass of the porcine vocal fold mucosa increased by around $5\%\text{--}10\%$ with an hour of hydration in an isotonic solution (incubation in Krebs-Ringer solution at $\text{pH} 7.4$). This discrepancy in specimen mass could indeed introduce a larger variability into the stress-strain data, as mass affects the calculation of cross-sectional area of the specimen. However, based on our animal data the increase in variability was limited to only about 5% of the specimen mass before incubation, resulting in a 5% or less error in the calculated stress values. The nominal stress was selected as a stress measure in order to facilitate the comparison to previously published data on the vocal ligament and the vocal fold body (muscle).⁸ This definition of stress is also commonly used in other studies in soft tissue biomechanics.^{15,16,21} Each specimen was loaded to a

constant value of maximum length at load reversal l_{rev} such that the stretch at load reversal is defined as $\lambda_{u,rev}=l_{rev}/L$.

Vocal fold cover specimens were dissected from 11 larynges excised within about 24 h postmortem, procured from autopsy from human cadavers free of head and neck disease and laryngeal pathologies. All subjects were nonsmokers and were Caucasians, although race was never a factor in the procurement. Tissue samples were obtained from six male larynges of ages $Y=17, 33, 51, 65, 66,$ and 99 years. The vocal fold *in situ* lengths of the male specimens were $L=14.1, 17.8, 22.4, 18.0, 20.4,$ and 17.0 mm, respectively, in the order of increasing subject age. The *in situ* lengths of male specimens did not significantly depend on age ($p=0.58$). Exploiting the displacement range of the lever system the male specimens were loaded to stretches of up to $\lambda_{u,rev}=1.35$. Samples were obtained also from five female larynges of ages $Y=80, 82, 83, 85,$ and 97 years. The vocal fold *in situ* lengths of the female specimens were $L=14.5, 14.9, 15.1, 13.7,$ and 13.9 mm, respectively, in the order of increasing subject age. The *in situ* lengths of female specimens did not significantly depend on age ($p=0.31$). Female specimens possess shorter *in situ* lengths than male specimens at a level of statistical significance ($p=0.02$). Exploiting the displacement range of the lever system, the female specimens were loaded to stretches of up to $\lambda_{u,rev}=1.5$ except for the specimen $Y=97$ which was tested to smaller maximum deformation.

In the experiments, the goal was to prevent any slackness in the sutures and to mount the specimen at a length as close to its *in situ* length as possible. No further pre-deformation was used in the experiments. The *in situ* length was used as the reference length for calculation of stretch values. Mounting was accomplished such that a tensile force of $0.01-0.02$ N was applied to the specimen. This force relaxed until the start of each test. The stress-stretch curves reported are those after preconditioning, i.e., after the stretch-release loading had reached a stable response. A stabilized response was typically achieved after 10 to 12 cycles. During preconditioning the experimental data shifted from the initial zero position of the load-elongation diagrams due to creep deformation. For the analysis of the experimental data in the preconditioned state and their characterization by the constitutive model the creep offset deformation was subtracted and load-elongation curves were placed at zero.

Measured tensile stress-stretch curves obtained for the male and female specimens are given in Fig. 3. While only a limited number of specimens are available, all curves show similar characteristics. A significant hysteresis and a strong nonlinear dependence of stress on the applied stretch is observed, similar to previous stress-strain data on the human vocal ligament.⁸ For higher stretch values the fit is still good but less perfect. This is attributed to potential heterogeneous deformation at larger magnitudes of deformation.

B. Constitutive characterization

The constitutive model is applied to characterize each of the specimens with the multi-parameter constitutive model. The resulting constitutive material parameters

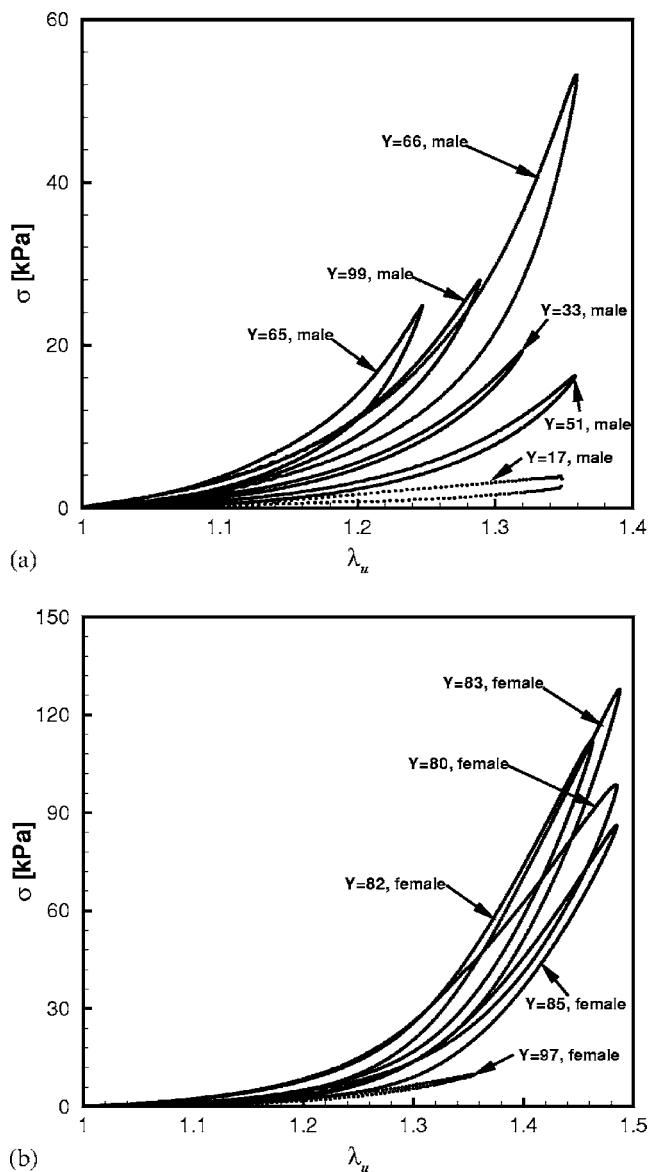


FIG. 3. Experimental tensile stress-stretch response at loading frequency of 1 Hz: (a) male vocal fold cover specimens and (b) female vocal fold cover specimens (Y =age in years).

$\mu_A, \alpha, \mu_B, Z, m, c$ obtained for the individual specimens are subsequently investigated in their age and gender differences. The Appendix describes the procedure to determine the values of the constitutive parameters.

Figure 4 shows examples of specimen response in the constitutive model in comparison to experimental data for two male and two female samples, respectively. The two male examples $Y=17$ and 99 are chosen to document in detail the differences in tissue response between a very young subject and one of advanced age, and to demonstrate the flexibility of the constitutive model to characterize significantly different types of stress-stretch response in a unified framework. It can be seen from Fig. 4(a) that the samples for the male subjects $Y=17$ and 99 exhibit quite significantly different characteristics with respect to hysteresis and the stress level associated with an applied level of deformation. Such differences are interpreted as possibly age related, due to the ultrastructural changes occurring with age,^{23,24} as in

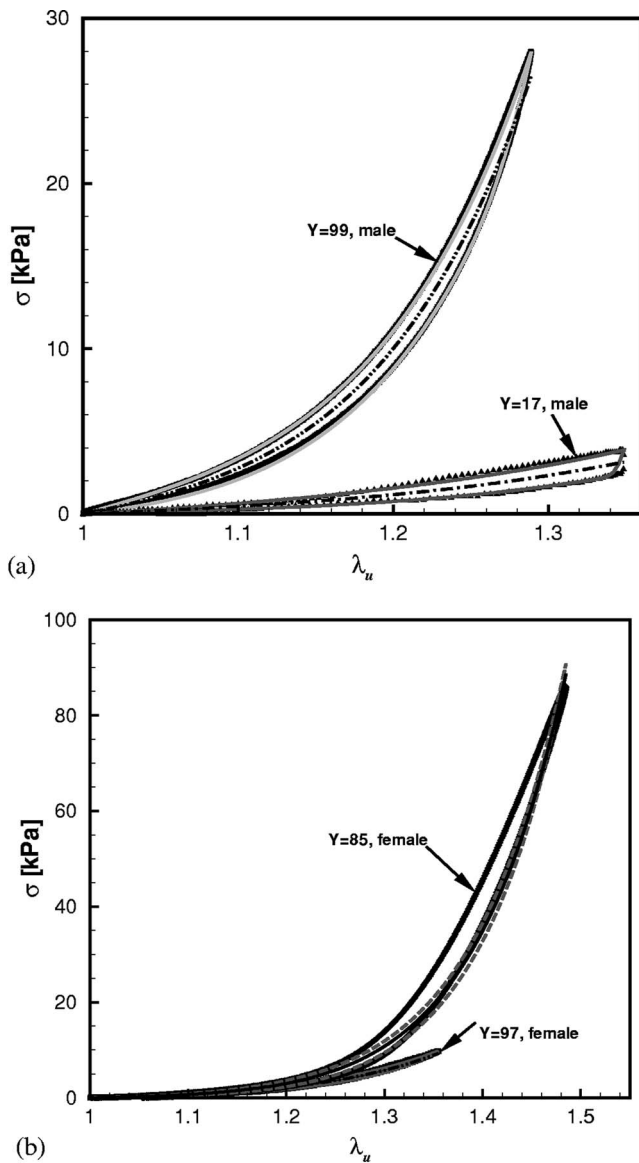


FIG. 4. Comparison between experimental data (—) and simulation results (—) of tensile stress-stretch response at 1 Hz: (a) male specimens $Y=17$ and $Y=99$ and (b) female specimens $Y=85$ and $Y=97$.

some other human soft tissues such as lung tissue.³⁴ Despite these differences the constitutive model can characterize both stress-stretch curves well. Parameter values of the constitutive parameters for all male subjects are summarized in Table I. For all samples the experimental data and the model

characterization were highly correlated ($R^2 \geq 0.9792$), indicating the capability of the constitutive model to describe the stabilized hysteretic tissue response, at least among the limited number of specimens examined. The two female samples depicted in Fig. 4(b), $Y=97$ and 85 , are chosen due to the difference in the maximum applied stretch level, $\lambda_{u,rev}=1.35$ for $Y=97$ and $\lambda_{u,rev}=1.48$ for $Y=85$. For the 97-year-old specimen, a good agreement between experimental data and constitutive description is obtained over the entire range of stretch, with $R^2=0.9976$. For the female specimen $Y=85$, and similarly for all other female specimens, the hysteretic response at large stretches, $\lambda_u > 1.3$, is not as well approximated as for moderate values of stretch, $\lambda_u < 1.3$. While the peak stress at load reversal is well predicted, the current model tends to underpredict the magnitude of the hysteresis observed experimentally. The parameter values of the constitutive model for the case of female subjects are also summarized in Table I. The R^2 values indicate a good approximation of the experimental data by the constitutive model, especially for $\lambda_u < 1.3$.

C. Age- and gender-related differences in tissue behavior

For male specimens it was possible to establish a relationship between the tissue response and age. A nonlinear regression analysis³⁵ was conducted for the parameter values of the equilibrium network (A) μ_A and α . Both data sets could be fitted with exponential functions: $\mu_A(Y)=7.0[1.0 - \exp(-0.01884Y)]$, with the regression coefficient $R^2=0.615$, and $\alpha(Y)=15.35[1.0 - \exp(-0.05841Y)]$, with $R^2=0.8744$. The individual data for μ_A and α , together with the exponential regression functions and the corresponding 95% confidence intervals, are given in Figs. 5(a) and 5(b). The value of μ_A , i.e., the stiffness of the tissue equilibrium response, increases with age, with the increase more significant in the age range below 65 years of age and a saturation at older age. The regression data suggest that μ_A for older males is up to three times larger than that of young adult males. Similarly, the nonlinearity of the tissue hyperelastic response, as characterized by the power α in the Ogden model, also increases with age [Fig. 5(b)]. This effect seems to be more significant in the age range below 50 years of age and again appears to saturate at older age. The present data suggest that the value of α increases by approximately a factor of 2 from young adult males to old males. The age

TABLE I. Summary of the parameters of the constitutive model and R^2 values for comparison of experimental data and constitutive description.

	Male specimens						Female specimens				
Age	17	33	51	65	66	99	80	82	83	85	97
μ_A (kPa)	1.37	3.50	1.765	6.67	5.6	6.39	4.117	3.63	1.307	1.426	1.77
α	8.8	14.1	14.6	16.1	14.5	14.4	14.54	15.44	19.47	16.83	12.5
μ_B (kPa)	80	20	25	60	130	40	190.0	70.0	180.0	60.0	10.0
m	1.5	1.8	1.2	1.6	1.6	2.1	1.1	1.7	1.0	1.0	1.3
c	-1.0	-1.0	-1.0	-1.0	-1.0	-1.0	-1.0	-1.0	-1.0	-1.0	-0.7
$Z[s^{-1}(kPa)^{-m}]$	6.0e-2	9.0e-2	5.0e-2	6.5e-3	3.4e-3	1.0e-2	8.0e-3	1.0e-2	8.0e-3	3.5e-2	2.0e-1
R^2 ($\lambda_u < 1.3$)							0.991	0.990	0.889	0.985	0.993
R^2 (entire curve)	0.979	0.999	0.999	0.999	0.998	0.999	0.908	0.991	0.520	0.987	0.997

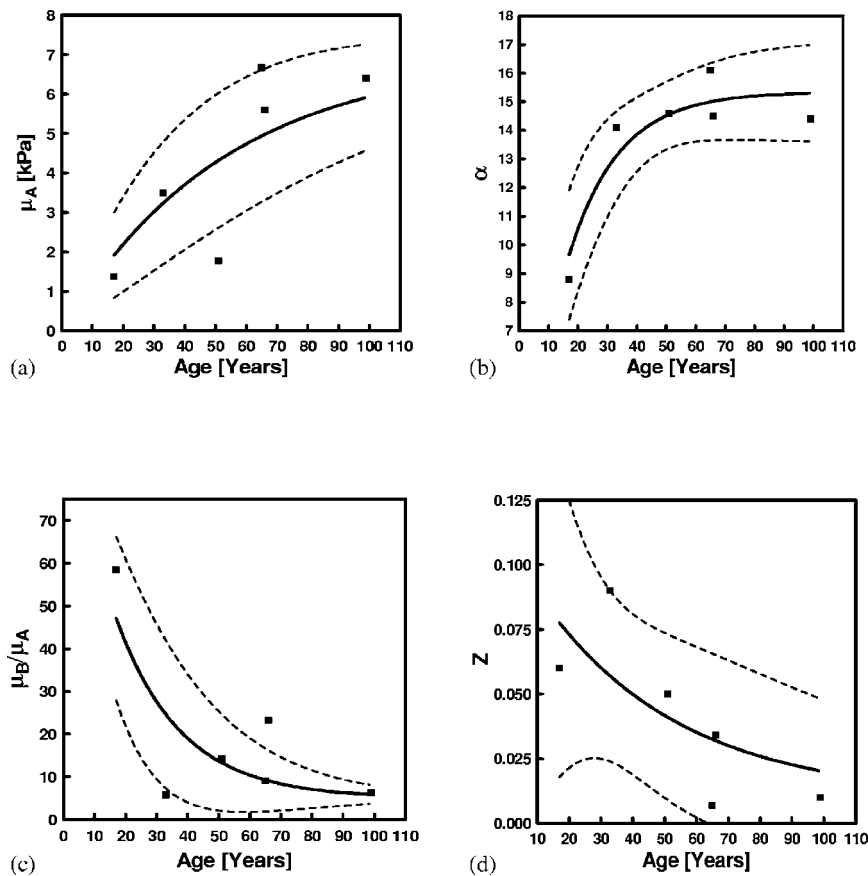


FIG. 5. Age dependence of the model parameters for the male specimens: (a) initial shear modulus of the equilibrium network (μ_A), (b) power in the Ogden model (α), (c) ratio between the stiffness of the time-dependent network relative to the stiffness of the equilibrium network (μ_B/μ_A), and (d) the viscosity scaling constant (Z). Dotted lines are the 95% confidence intervals of the curve-fitting exponential functions.

dependence of the ratio between the initial shear modulus of the time-dependent network (B) μ_B relative to the initial shear modulus of the equilibrium network (A) μ_A is given in Fig. 5(c) together with a nonlinear regression function and the corresponding 95% confidence intervals. The exponential function $\mu_B/\mu_A = 95.0 \exp(-0.04785Y) + 5.0$ provides a reasonable fit to the experimental data with a regression coefficient of $R^2 = 0.6625$. It should be noted here again that the same value of α was used for both network (A) and network (B) in the model. For the dependence of the effective inelastic stretch rate on the effective inelastic stretch, a single value of the parameter c was used throughout the study, i.e., $c = -1.0$, and hence there was no age dependence for this parameter. The stress dependence of the inelastic deformation as expressed through the power m was found to not significantly vary with age. The mean value of this parameter was determined as $\bar{m} = 1.633$ with a standard deviation of 0.3011. A one-sample two-tailed t test was conducted to verify if the stress dependence of the viscoplastic flow law was significantly different from $m = 0$. This test resulted in a p value of $p < 0.0001$, demonstrating statistical significance. The finding that m can be assumed as a constant is especially interesting when considering the analysis of the age dependence of the viscosity scaling constant Z . A comparison of the values of this parameter becomes meaningful if m can be treated as a constant, such that all Z values possess the same units, i.e., $\sim [s^{-1}(\text{kPa})^{-1.6}]$ in the present case. Figure 5(d) depicts the age dependence of Z together with the nonlinear regression function and the corresponding 95% confidence intervals. The nonlinear regression analysis led to an expo-

ponential function of $Z(Y) = 0.0998 \exp(-0.0229 \cdot Y) + 0.01$, with $R^2 = 0.5504$. Figure 5(d) suggests that the viscous response of the tissue, as characterized by Z , decreases significantly with age. For older males Z is found to be approximately one-third of that of young adult males.

For the female specimens no age dependence could be determined due to the small spread in age in the specimens available. Nevertheless, the dependence of the constitutive parameters on gender is investigated. For female subjects the mean age is $\bar{Y} = 85$ compared to $\bar{Y} = 55$ for the male subject group. In order to examine gender-related effects in subjects of a similar age range, the two youngest male specimens were excluded from the analysis, resulting in $\bar{Y} = 70$ for the male subgroup. Following the results of Fig. 5, in this subgroup the age dependence of the model parameters is then much less pronounced than for the overall male population. For the female specimens a mean value of the tissue equilibrium stiffness of $\bar{\mu}_A = 2.45$ kPa with a standard deviation of 1.32 kPa was obtained, whereas for the male specimens ($\bar{Y} = 70$) it was $\bar{\mu}_A = 5.11$ kPa with a standard deviation of 2.27 kPa. These data result in a male-to-female difference in the mean values of tissue equilibrium stiffness of $\bar{\mu}_A(\text{male}) - \bar{\mu}_A(\text{female}) = 2.66$ kPa. A one-tailed t test was conducted to investigate if this difference between male and female tissue stiffness was statistically significant. This test resulted in a value of $p = 0.031$ (DOF = 4.591), indicating that this gender-related difference in stiffness was significant. In addition, a nonparametric Mann-Whitney U test was conducted to further investigate if the finding of $\bar{\mu}_A(\text{male}) > \bar{\mu}_A(\text{female})$ was

statistically significant, without the assumption of normal sample distribution. This test returned a value of $p=0.0557$, close to statistical significance. A similar analysis of gender-related difference was also conducted for the power of the hyperelastic response in the Ogden model. For the female specimens a mean value of $\bar{\alpha}=15.76$ with a standard deviation of 2.60 was obtained. For the male specimens ($\bar{Y}=70$) it was found that $\bar{\alpha}=14.90$ with a standard deviation of 0.4. These data result in a difference between male and female of $\bar{\alpha}(\text{male})-\bar{\alpha}(\text{female})=-0.856$. Results of both the t test and Mann-Whitney U test indicate that the difference was not statistically significant with $p>0.5$ in both cases.

For the parameters characterizing the inelastic tissue response no further statistically significant gender difference was observed: for μ_B/μ_A a one-tailed t test for significance in gender resulted in $p=0.093$ (DOF=4.207); the corresponding U test for $\mu_B/\mu_A(\text{male})>\mu_B/\mu_A(\text{female})$ resulted in $p=0.143$. For m a one-tailed t test for significance in gender resulted in $p=0.063$ (DOF=5.733), and the corresponding U test for $m(\text{male})>m(\text{female})$ resulted in $p=0.087$. For Z a two-tailed t test for significance in gender resulted in $p=0.415$ (DOF=4.67), and the corresponding U test for $Z(\text{male})<Z(\text{female})$ resulted in $p=0.2293$.

IV. ANALYSIS OF THE EQUILIBRIUM F_0

Predictions of fundamental frequency can be obtained from Eqs. (1) and (2) once a constitutive model is established and its parameter values are determined. For comparison purposes, the example of linear elasticity as described by Hooke's law is considered first. Combining a one-dimensional description of linear elasticity model, $\sigma=E\epsilon =E(\lambda_u-1)$, with Eq. (2) one obtains

$$F_{0,\text{lin}} = F_{\text{lin}}^* \frac{\sqrt{\lambda_u-1}}{\lambda_u} [1 - 0.45 \ln(\lambda_u - 1)] \quad (13)$$

with

$$F_{\text{lin}}^* = \frac{\sqrt{E}}{2L\sqrt{\rho}}. \quad (14)$$

The fundamental frequency F_0 is thus given as the product of a deformation measure and a reference frequency F_{lin}^* containing the information of the tissue elastic response, its resting length and density.

For the hyperelastic tissue response the combination of Eq. (2) with Eq. (10) leads to a prediction of $F_{0,\text{hyper}}$ in dependence of the constants of the hyperelastic constitutive model and the tensile deformation as

$$F_{0,\text{hyper}} = F_{\text{hyper}}^* \sqrt{\lambda_u^{\alpha-3} - \lambda_u^{-\alpha/2-3}} [1 - 0.45 \ln(\lambda_u - 1)] \quad (15)$$

with

$$F_{\text{hyper}}^* = \frac{\sqrt{2\mu_A}}{2L\sqrt{\rho\alpha}}. \quad (16)$$

The influence of vocal fold deformation on fundamental frequency is assessed by plotting the normalized fundamental frequency F_0/F^* as a function of vocal fold length changes as characterized by stretch λ_u (Fig. 6). For the linear elastic

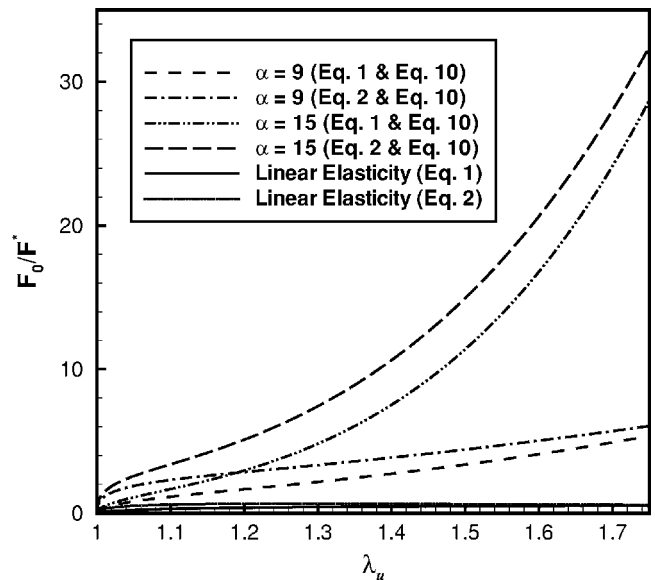
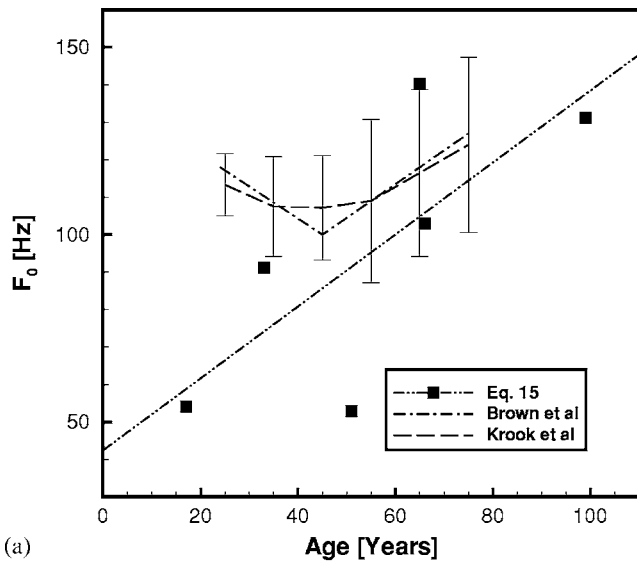


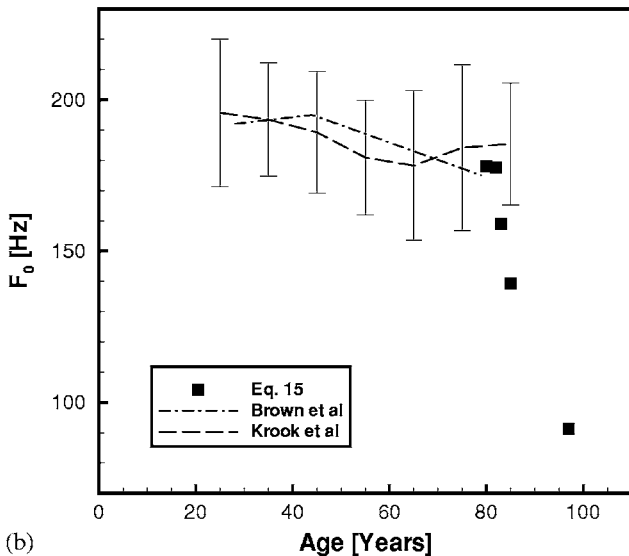
FIG. 6. Dependence of the predicted normalized fundamental frequency F_0/F^* on applied tensile stretch λ_u based on Eqs. (10) and (16). Predictions are shown for a young adult male ($\alpha=9.0$), an old adult male ($\alpha=15.0$), and a linear elastic model (Hooke's law).

model the predicted values of F_0/F^* are only slightly dependent on the applied stretch and become nearly constant for $\lambda_u > 1.2$, independently of whether the correction proposed by Titze and Hunter²⁵ is included or not. This is in significant contrast to results of *in vivo* observations of human vocal fold length during pitch changes.³⁶ Much better qualitative agreement with the observations of Ref. 36 is obtained with the predictions of F_0/F^* from the hyperelastic model. F_0/F^* depends nonlinearly on λ_u and strongly increases with vocal fold stretch. The change in the value of the parameter α significantly influences the dependence of F_0/F^* on λ_u . For larger values of α ($\alpha=15.0$ typical of subjects of advanced age in the male group) F_0/F^* depends more strongly on stretch than for low values of α ($\alpha=9.0$ typical of young males). Again, these trends are independent of whether the correction function of Titze and Hunter²⁵ is included or not.

The predicted dependence of F_0 on age for the male specimens is depicted in Fig. 7(a) with F_0 calculated through Eq. (15). For the calculation of F_0 , individual specimen resting length data were combined with the constitutive parameters given in Table I. A stretch of $\lambda_u=1.2$ —typical length changes in males—and a tissue density of $\rho=1040 \text{ kg/m}^3$ were assumed.^{5,36} To put predicted F_0 data into perspective, Fig. 7(a) also shows trend-lines approximating the life-span changes of F_0 based on human speaking F_0 data obtained by Brown *et al.*³⁷ and Krook³⁸ A linear regression analysis was conducted, and it was found that the predicted F_0 could be fitted by $F_0(Y)=0.9599Y+42.454$, with the regression coefficient $R^2=0.55$. The present finding of an age-related increase in fundamental frequency due to changes in the hyperelastic constitutive parameters is consistent with empirical life-span changes after middle age where F_0 gradually increases with age in males above $Y \approx 40$.³⁷⁻³⁹



(a)



(b)

FIG. 7. Dependence of the predicted fundamental frequency F_0 on age for (a) male specimens and (b) female specimens. Data points represent individual specimens of the present study. Two trend-lines depict approximately the change in speaking fundamental frequency with age as reported by Brown *et al.*³⁷ and Krook³⁸

In females, the data of Brown *et al.*³⁷ and Krook³⁸ show a gradual decrease of F_0 on age, especially for Brown *et al.*³⁷ They also found F_0 to be larger in females than in males, as expected. Equation (15) was also used to predict F_0 values for the present female subjects. Again, for this analysis individual specimen resting length data were combined with the constitutive parameters given in Table I, and a tissue density of $\rho=1040 \text{ kg/m}^3$ was assumed. However, for the female subjects a larger value of stretch due to posturing was used, $\lambda=1.3$.³⁶ Figure 7(b) depicts trends of F_0 from Refs. 37 and 38 in comparison to predicted F_0 values. For several of the subjects, the predicted F_0 is well in the range of data from Refs. 37 and 38, while for the oldest female subject ($Y=97$) the predicted F_0 value is much lower.

In general, the values of F_0 predicted in the present study tend to be lower than those from speaking data. Several factors are deemed responsible for this. First, the inelastic tissue properties need to be considered. For a discussion of this aspect, see the following section. Second, only the vocal fold cover is investigated in the present study. The use of Titze and Hunter's²⁵ correction factor is only a rough approximation for our description of the vocal fold cover, since it was derived for the vocal ligament. The effect of bending stiffness is expected to be similar, but not the effect of the macula flavae, which are not part of the vocal fold cover. Future studies should include a correction factor more specific to the vocal fold cover, as well as the key contributions of the vocal ligament, which should allow the model to predict more physiological F_0 values. Third, intrinsic laryngeal muscle activities were not included in the present study. Activities of the cricothyroid and the thyroarytenoid muscles could either increase or decrease the stiffness of the vocal fold cover depending on a balance of their antagonistic actions, and it is well documented that they combine to regulate F_0 .^{39,40}

V. ANALYSIS OF THE NONEQUILIBRIUM F_0

In the results presented in the preceding section the analysis of F_0 was based only on the hyperelastic contribution of the equilibrium network (A). If Eq. (15) was calculated with $\mu_A + \mu_B$ instead of μ_A only, values of F_0 much larger than physiological data would be predicted. For example, for males $Y > 50$ an average value of $\bar{F}_0 = 388 \text{ Hz}$ is obtained at $\lambda_u = 1.2$. This finding suggests that the elastic component of network (B) may only partially be contributing to the regulation of F_0 . The exact relative amount of elastic and inelastic deformation in network (B) depends on the frequency and the magnitude of the stretch during vocal fold length changes. Predictions of the time-dependent evolution of F_0 can be obtained by combination of Eq. (2) with numerical predictions of the longitudinal tissue stress by use of solutions from Eq. (12). One example of a predicted time dependence of F_0 is given in Fig. 8 where a deformation history of $\lambda_u = 1.0 \rightarrow 1.2 \rightarrow \text{hold} \rightarrow 1.1 \rightarrow \text{hold} \rightarrow 1.2 \rightarrow \text{hold} \rightarrow 1.1$ is considered. The stretch rate in the computation is $0.4/\text{s}$ such that the initial stretch takes 0.5 s corresponding to a loading frequency of 1 Hz . Such rates of stretch are representative of vocal fold length changes during speech.³¹⁻³³ The present model predicts changes in F_0 to occur over short time periods (several ms to several hundred ms) after stretch was changed. If stretch is increased from the previous level, F_0 drops from a higher value to a steady state. If stretch is decreased from the previous level, F_0 increases from a lower value to a steady state. The findings of predicted F_0 changes to occur in the range of up to several hundred milliseconds are in general agreement with exponential time constants for vocal fold length changes if they occurred at submaximal speeds.³³

In order to quantify the time-dependent response, we define a characteristic time constant as the time for 90% of stress relaxation to have occurred. Figures 9(a) and 9(b) show predicted time constants for male and female speci-

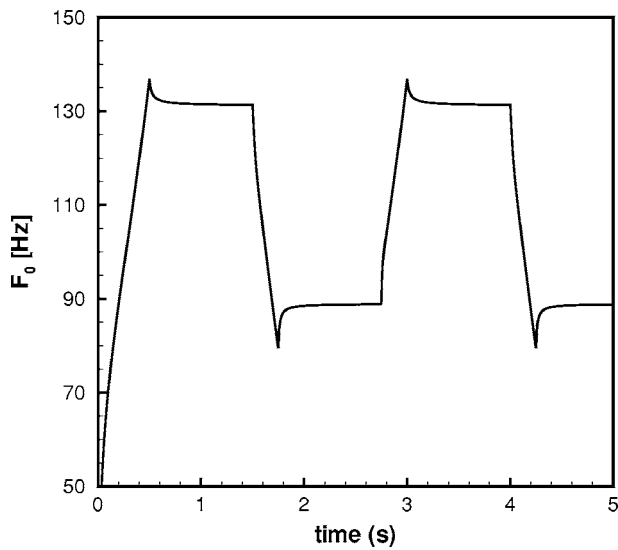
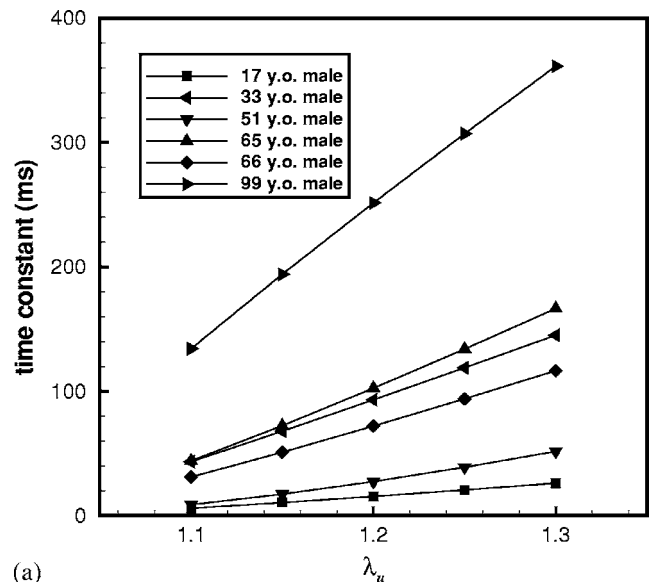


FIG. 8. Predicted time course of F_0 for a stretch history $\lambda_u=0 \rightarrow 1.2 \rightarrow 1.1 \rightarrow 1.2 \rightarrow 1.1$ and a loading frequency of 1 Hz. Simulation conducted with constitutive parameters of the 99-year-old male specimen with ($Y=99$).

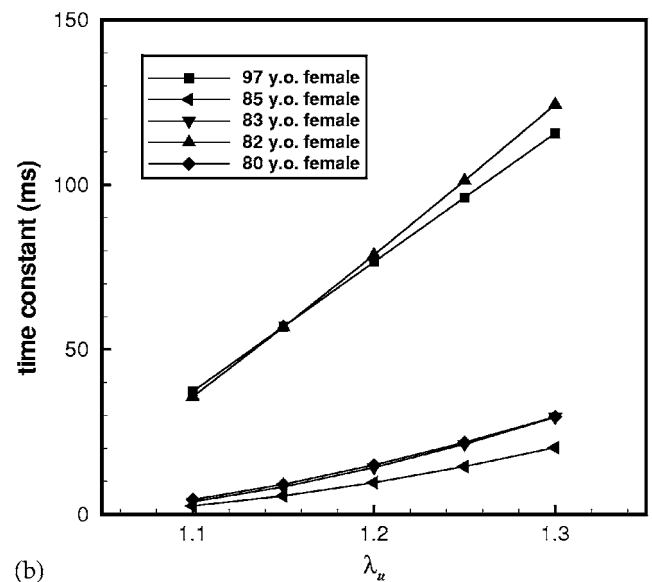
mens, respectively, in dependence of applied stretch. The predicted time constants are found to be dependent on stretch. As stretch increases the inelastic response of the tissue is reduced and the time required for stress relaxation increases. For male subjects the characteristic time constant at $\lambda_u=1.2$ increases with age, $\tau=1.2 \times 10^4 + 4.0[1 - \exp(-0.00011 \times Y)]$, $R^2=0.605$. However, no statistically significant difference between gender was found.

VI. DISCUSSION

The present study documents the large-strain, hyperelastic, and viscous (hysteretic) response of the human vocal fold cover under uniaxial tensile deformation. Experimental stress-stretch (or stress-strain) data were obtained from the superficial layer of the lamina propria (the vocal fold cover), as compared to previous data on the deeper layers of the lamina propria (the vocal ligament).⁸ Both the epithelium and the superficial layer of the lamina propria likely contributed to the observed tensile mechanical response, although it was not possible to determine their exact contributions in the present study. In agreement with previous studies on vocal fold elasticity, it was found that the vocal fold cover was highly nonlinear, hysteretic, and with a large interindividual variability, although these observations were based on only a limited number of specimens. To obtain a more fundamental understanding of the structural basis of the tissue deformation response based on age- and gender-related differences, a constitutive modeling approach was employed in the analysis of the data. The constitutive model was formulated based on the application of Ogden's hyperelastic model within an incremental inelastic (viscoplastic) network model. In this constitutive formulation, no arbitrary separation into a low-strain, linear elastic region and a large-strain, nonlinear exponential regime is required, as was common in earlier studies of vocal fold tissue elasticity.^{7,8} Results showed that the constitutive model approach was capable of simulating the vocal fold cover deformation response if the applied de-



(a)



(b)

FIG. 9. Predicted dependence of the characteristic time constant of relaxation on the applied stretch for (a) male specimens and (b) female specimens. Loading frequency=1 Hz.

formation remained below a stretch of $\lambda < 1.3$. For higher values of the applied stretch it appears that more than one inelastic mechanism of deformation needs to be accounted for, particularly for characterizing the female specimens. An extension of the current model to allow for its application at large deformation can be constructed by adding a second inelastic network to the model, for example. Such an approach is currently under investigation.

From a functional biomechanical perspective it is of great interest to correlate the tissue mechanical response to the histological structure of the vocal fold ECM. For the human vocal fold age- and gender-dependent variations in collagen and elastin concentrations and their spatial distributions in the lamina propria were reported by Hammond *et al.*^{23,24} Collagen concentration in the most superficial 40% of the lamina propria (cover) was observed to increase with age for males, but was found to be rather constant with age

for females. On the other hand, elastin concentration in the vocal fold cover was observed to increase with age for both males and females. When comparing the collagen content between geriatric males and females of 65 to 82 years of age, it was found that the collagen concentration in the vocal fold cover of males was considerably larger than in samples of females, whereas for elastin it was smaller in geriatric males than in females.^{23,24} In the present study, for the male specimens it was possible to correlate the tissue mechanical response as expressed by the parameters of the constitutive model to their age. Consistent with the age-related increase in collagen and elastin concentrations it was observed that the tissue stiffness-characterizing parameters, μ_A and α , generally increase in magnitude with increasing age. These changes in tissue properties are well represented in the predicted fundamental frequency response, i.e., the increase of the predicted F_0 is correlated with the increase in the magnitude of the stiffness characterizing parameters.

In addition, the response of the male and the female specimens was compared with respect to the stiffness of the time-independent equilibrium response in network (A), i.e., $\bar{\mu}_A$. The present data suggest that stiffness of the male vocal fold cover is approximately twice that of the female, consistent with a higher collagen concentration (and perhaps lower elastin concentration) in geriatric males. Due to the small number of samples available within each gender group, however, this finding needs to be considered as preliminary, even though results of the t test indicated the difference was statistically significant. The parameter α determines the degree of nonlinearity of the tissue hyperelastic response, and its value qualitatively depends on the process of the recruitment of collagen and elastin fibers into the loading direction.⁴¹ The lack of gender-related difference in $\bar{\alpha}$ could imply that the recruitment of collagen and elastin fibers in the vocal fold ECM to withstand tensile deformation is apparently gender unspecific. This was surprising, given that the male vocal fold cover has more collagen and less elastin than the female in geriatric specimens.^{23,24} Further studies with additional specimens are needed to resolve this apparent discrepancy. In considering the consequent gender differences in F_0 , gender-related magnitudes of vocal fold length changes are relevant. Adopting the finding that $\bar{\alpha}(\text{male}) \approx \bar{\alpha}(\text{female})$, $\bar{L} = 19.45$ mm (males, $Y > 50$) and $\bar{L} = 14.42$ mm (females), equal tissue densities for male and female, and a stretch of $\lambda_u = 1.2$, Eq. (15) predicts similar fundamental frequencies for the two genders, $\bar{F}_0(\text{male}) = 106$ Hz and $\bar{F}_0(\text{female}) = 104$ Hz. This finding suggests that the effect of longer vocal folds in our male specimens, which should lower F_0 , is being compensated for by their higher tissue stiffness, which raises F_0 . The higher F_0 values for females as documented from speech data could thus be the result of higher levels of stretch during vocal fold posturing.

The parameters characterizing the time-dependent response, μ_B and Z , decrease in magnitude with age. These parameter changes suggested that younger males may possess a compliant equilibrium network (A) and a relatively high stiffness in the elastic response of network (B). In such a situation, most of the stress would be carried by the net-

work (B). Since the viscosity scaling constant Z of the inelastic flow rule was also large for the younger males, the resulting amount of inelastic deformation would be significant and lead to a pronounced hysteretic response. Older males may possess a stiffer equilibrium network (A) and a relatively compliant elastic response in network (B). In this case a reduced level of stress would be present in the time-dependent network (B). Since the viscosity scaling constant Z of the inelastic flow rule was small, the resulting amount of inelastic, time-dependent deformation would be reduced. This trend is represented in the increase in the value of the predicted time constants with age (Fig. 9).

VII. CONCLUSION

The mechanical behavior of the human vocal fold cover under large-strain uniaxial tensile loading was quantified at a frequency of 1 Hz, and data for six male and five female specimens were obtained. While this data set is limited and the findings should be considered preliminary, several conclusion could nonetheless be drawn:

- (1) The stress-strain response of the vocal fold cover was found to be highly nonlinear and hysteretic, consistent with previous findings on vocal fold elasticity. Age and gender of the specimens appeared to significantly impact both the elastic and the time-dependent tensile deformation behavior. A constitutive model approach comprised of a hyperelastic (large-strain), equilibrium network in parallel with an inelastic (viscoplastic), time-dependent network was formulated to simulate the empirical data. It was found that the model was capable of describing the tissue behavior with reasonably high confidence, except for high levels of vocal fold elongation.
- (2) Trends found in the age and gender dependence of the tissue mechanical behavior are in good agreement with previously reported age- and gender-related differences of collagen and elastin concentrations in the vocal fold cover. Based on the constitutive parameters it was found that for males the stiffness of the time-independent response increases with age and that the viscous hysteretic response of the tissue decreases with age. When comparing the gender groups, geriatric male specimens appeared to be nearly twice as stiff as the geriatric females. No significant difference between gender was found in the time-dependent response.
- (3) Predictions of the fundamental frequency showed an increase in this parameter with age for males, in agreement with published life-span changes of F_0 . The predicted characteristic time constants for F_0 under stretch transients are in the range of those from speech data. The magnitude of the time constants tends to increase with age.
- (4) Considering equal magnitude of stretch, similar fundamental frequencies between geriatric males and females are predicted as the effect of shorter vocal fold length in females is compensated for by the reduced

tissue stiffness. No significant difference in the time-dependent response between males and females was found.

This study has focused on only the passive biomechanical response of the vocal fold cover, without including the important contributions of the vocal ligament in tensile stress regulation, and the active contributions of the intrinsic laryngeal muscles. Also, the size of our empirical data pool was limited. Nevertheless, it was demonstrated that some of the empirical life-span changes of speaking F_0 could be explained by the proposed constitutive model reasonably well. The present findings suggest that our modeling approach may provide a promising framework for characterizing the contributions of the passive tissue mechanical response to the process of F_0 regulation. Future investigations should include a larger number of specimens, a constitutive model including an extended formulation of inelastic deformation, and considerations regarding the contributions of the vocal ligament to fundamental frequency.

ACKNOWLEDGMENTS

This work was supported by the National Institute on Deafness and Other Communication Disorders, NIH Grant No. R01 DC006101. The authors thank Neeraj Tirunagari and Min Fu of UT Southwestern Medical Center for their assistance in empirical measurements of vocal fold tissue elasticity.

APPENDIX

The procedure followed in the parameter identification follows Ref. 18 but incorporates modifications for the current choice of the hyperelastic response. Initially, stresses in network (B) are set to zero (fully relaxing the network) by assigning a large viscosity scaling constant Z ($Z > 1.0$). Then, the hyperelastic equilibrium response provided by network (A) becomes the model response, characterized by the parameters μ_A and α . The values of μ_A and α are determined through a least-square optimization process following the Levenberg-Marquardt method to best fit the experimental equilibrium response estimated from the empirical stress-stretch curves as the midpoint values between the loading and unloading portions of the hysteresis loop. Subsequently, the initial shear modulus of network (B) is determined from the tangent stiffness E_t at load reversal where network (B) responds through its hyperelastic deformation only. The tangent modulus at the onset of unloading E_t is the sum of the elastic moduli of the two networks:

$$E_t = 3\mu_B + \frac{2\mu_A}{\alpha} \left[(\alpha - 1)\lambda_{rev}^{\alpha-2} + \left(\frac{\alpha}{2} + 1\right)\lambda_{u,rev}^{-\alpha/2-2} \right]. \quad (A1)$$

The viscosity scaling constant Z is then obtained such that the simulated loading-unloading curves expand gradually from the equilibrium curve to fit the experimental data points of the stress-stretch hysteresis loop. The stress power parameter m is chosen such that the predicted response fits the initial slope of the experimental loading curves. For all but one of the present specimens of the present investigation

the stretch power parameter is set to $c = -1.0$. With this choice the model allows one to predict the decay in hysteretic loss with an increase in $\lambda_{u,rev}$ as observed previously.⁴

- ¹E. J. Hunter, I. R. Titze, and F. Alipour, "A three-dimensional model of vocal fold abduction/adduction," *J. Acoust. Soc. Am.* **115**, 1747–1759 (2004).
- ²I. R. Titze, J. G. Švec, and P. S. Popolo, "Vocal dose measures: Quantifying accumulated vibration exposure in vocal fold tissues," *J. Speech Lang. Hear. Res.* **46**, 919–932 (2003).
- ³I. R. Titze, "On the relation between subglottal pressure and fundamental frequency in phonation," *J. Acoust. Soc. Am.* **85**, 901–906 (1989).
- ⁴R. W. Chan and T. Siegmund, "Vocal fold tissue failure: preliminary data and constitutive modeling," *J. Biomech. Eng.* **126**, 466–474 (2004).
- ⁵F. Alipour, D. A. Berry, and I. R. Titze, "A finite-element model of vocal-fold vibration," *J. Acoust. Soc. Am.* **108**, 3003–3012 (2000).
- ⁶H. E. Gunter, "A mechanical model of vocal-fold collision with high spatial and temporal resolution," *J. Acoust. Soc. Am.* **113**, 994–1000 (2003).
- ⁷F. Alipour-Haghighi and I. R. Titze, "Elastic models of vocal fold tissues," *J. Acoust. Soc. Am.* **90**, 1326–1331 (1991).
- ⁸Y. B. Min, I. R. Titze, and F. Alipour-Haghighi, "Stress-strain response of the human vocal ligament," *Ann. Otol. Rhinol. Laryngol.* **104**, 563–569 (1995).
- ⁹T. Y. Hsiao, C. L. Wang, C. N. Chen, F. J. Hsieh, and Y. W. Shau, "Elasticity of human vocal folds measured *in vivo* using color Doppler imaging," *Ultrasound Med. Biol.* **28**, 1145–1152 (2002).
- ¹⁰A. P. Lobo and M. O'Malley, "A nonlinear finite-element model of the vocal fold," *J. Acoust. Soc. Am.* **99**, 2473–2500 (1996).
- ¹¹R. W. Chan and I. R. Titze, "Viscoelastic shear properties of human vocal fold mucosa: Measurement methodology and empirical results," *J. Acoust. Soc. Am.* **106**, 2008–2021 (1999).
- ¹²R. W. Chan and I. R. Titze, "Viscoelastic shear properties of human vocal fold mucosa: Theoretical characterization based on constitutive modeling," *J. Acoust. Soc. Am.* **107**, 565–580 (2000).
- ¹³M. S. Green and A. V. Tobolsky, "A new approach to the theory of relaxing polymeric media," *J. Chem. Phys.* **14**, 80–92 (1946).
- ¹⁴R. W. Ogden, "Larger deformation isotropic elasticity – on the correlation of theory and experiment for incompressible rubberlike solids," *Proc. R. Soc. London, Ser. A* **326**, 565–584 (1972).
- ¹⁵K. Miller and K. Chinzei, "Mechanical properties of brain tissue in tension," *J. Biomech.* **35**, 483–490 (2002).
- ¹⁶D. F. Meaney, "Relationship between structural modeling and hyperelastic material behavior: application to CNS white matter," *Biomech. Model. Mechanobiol.* **1**, 279–293 (2003).
- ¹⁷J. S. Bergström and M. C. Boyce, "Constitutive modeling of the large strain time-dependent behavior of elastomers," *J. Mech. Phys. Solids* **46**, 931–954 (1998).
- ¹⁸J. S. Bergström and M. C. Boyce, "Constitutive modeling of the time-dependent and cyclic loading of elastomers and application to soft biological tissues," *Mech. Mater.* **33**, 523–530 (2001).
- ¹⁹J. S. Bergström and M. C. Boyce, "Large strain time-dependent behavior of filled elastomers," *Mech. Mater.* **32**, 627–644 (2000).
- ²⁰C. P. Buckley and D. C. Jones, "Glass-rubber constitutive model for amorphous polymers near the glass transition," *Polymer* **36**(17), 3301–3312 (1995).
- ²¹M. B. Rubin and S. R. Bodner, "A three-dimensional nonlinear model for dissipative response of soft tissue," *Int. J. Solids Struct.* **39**, 5081–5099 (2002).
- ²²J. E. Bischoff, E. M. Arruda, and K. Grosh, "A rheological network model for the continuum anisotropic and viscoelastic behavior of soft tissue," *Biomech. Model. Mechanobiol.* **3**, 56–65 (2004).
- ²³T. H. Hammond, S. D. Gray, and J. E. Butler, "Age- and gender-related collagen distribution in human vocal folds," *Ann. Otol. Rhinol. Laryngol.* **109**, 913–920 (2000).
- ²⁴T. H. Hammond, S. D. Gray, J. Butler, R. Zhou, and E. H. Hammond, "A study of age and gender related elastin distribution changes in human vocal folds," *Otolaryngol.-Head Neck Surg.* **119**, 314–322 (1998).
- ²⁵I. R. Titze and E. J. Hunter, "Normal vibration frequencies of the vocal ligament," *J. Acoust. Soc. Am.* **115**, 2264–2269 (2004).
- ²⁶S. D. Gray, I. R. Titze, R. Chan, and T. H. Hammond, "Vocal fold proteoglycans and their influence on biomechanics," *Laryngoscope* **109**, 845–854 (1999).
- ²⁷S. D. Gray, I. R. Titze, F. Alipour, and T. H. Hammond, "Biomechanical

- and histological observations of vocal fold fibrous proteins," *Ann. Otol. Rhinol. Laryngol.* **109**, 77–85 (2000).
- ²⁸MATLAB, The MathWorks, Inc., Natick, MA (Version 7.0).
- ²⁹A. L. Perlman, "A technique for measuring the elastic properties of vocal fold tissue," Ph.D. dissertation, The University of Iowa, Iowa City, IA, 1985.
- ³⁰S. D. Gray, K. J. Chan, and B. Turner, "Dissection plane of the human vocal fold lamina propria and elastin fibre concentration," *Acta Oto-Laryngol.* **120**, 87–91 (2000).
- ³¹J. Ohala and W. Ewan, "Speed of pitch change," *J. Acoust. Soc. Am.* **53**, 345A (1973).
- ³²J. Sundberg, "Maximum speed of pitch changes in singers and untrained subjects," *J. Phonetics* **7**, 71–79 (1979).
- ³³I. R. Titze, J. J. Jiang, and E. Lin, "The dynamics of length change in canine vocal folds," *J. Voice* **11**, 267–276 (1997).
- ³⁴S. J. Lai-Fook and R. E. Hyatt, "Effects of age on elastic moduli of human lungs," *J. Appl. Physiol.* **89**, 163–168 (2000).
- ³⁵J. Neter, M. H. Kutner, C. J. Nachtsheim, and W. Wasserman, *Applied Linear Statistical Models*, 4th ed. (McGraw-Hill, New York, 1996).
- ³⁶H. Hollien, "Vocal pitch variation related to changes in vocal fold length," *J. Speech Hear. Res.* **3**, 150–156 (1960).
- ³⁷W. Brown, R. Morris, Jr., H. Hollien, and E. Howell, "Speaking fundamental frequency characteristics as a function of age and professional singing," *J. Voice* **5**, 310–315 (1991).
- ³⁸M. I. P. Krook, "Speaking fundamental frequency characteristics of normal Swedish subjects obtained by glottal frequency analysis," *Folia Phoniatr.* **40**, 82–90 (1988).
- ³⁹I. R. Titze, *Principles of Voice Production* (Prentice-Hall, Englewood Cliffs, NJ, 1994).
- ⁴⁰M. Döllinger, D. A. Berry, and G. S. Berke, "Medial surface dynamics of an in vivo canine vocal fold during phonation," *J. Acoust. Soc. Am.* **117**, 3174–3183 (2005).
- ⁴¹P. Fratzl, K. Misof, I. Zizak, G. Rapp, H. Amenitsch, and S. Bernstorff, "Fibrillar structure and mechanical properties of collagen," *J. Struct. Biol.* **122**, 119–122 (1997).